View metadata, citation and similar papers at core.ac.uk

brought to you by CORE

provided by E-space: Manchester Metropolitan University's Research Repository

Manchester Metropolitan University

Potgieter, JH and Pardesi, C and Pearson, S (2020)A kinetic and thermodynamic investigation into the removal of methyl orange from wastewater utilizing fly ash in different process configurations. Environmental Geochemistry and Health. ISSN 0269-4042

Downloaded from: http://e-space.mmu.ac.uk/625749/

Version: Accepted Version

Publisher: Springer Science and Business Media LLC

DOI: https://doi.org/10.1007/s10653-020-00567-6

Usage rights: Creative Commons: Attribution 4.0

Please cite the published version

https://e-space.mmu.ac.uk

Environ Geochem Health
https://doi.org/10.1007/s10653-020-00567-6

ORIGINAL PAPER

A kinetic and thermodynamic investigation into the removal of methyl orange from wastewater utilizing fly ash in different process configurations

J. H. Potgieter · C. Pardesi · S. Pearson

Received: 8 January 2020 / Accepted: 10 April 2020
© The Author(s) 2020

Abstract The removal of methyl orange using coal fly ash, which is a widely available low-cost adsorbent, has been investigated. Adsorption studies for dye removal were conducted using various configurations such as batch, column and heap adsorption at various temperatures and adsorbent dosages at neutral pH. The Langmuir, Freundlich and Tempkin isotherm models were used to describe the process. The Freundlich model best represented the adsorption. Kinetic studies show the adsorption followed pseudo-second-order kinetics. Thermodynamic studies show that the process is spontaneous, endothermic and random. Column configuration was found to be the most efficient with a dye removal percentage of 99.95%, followed by heap adsorption at 99.25% removal and lastly batch configuration with 96.68% removal. Economic analysis shows that column operation would be the most effective for practical implementation.

Keywords Methyl orange · Coal fly ash · Adsorption studies · Batch · Column · Heap adsorption

J. H. Potgieter · C. Pardesi · S. Pearson
School of Chemical and Metallurgical Engineering, The University of the Witwatersrand, 1 Jan Smuts Avenue & Jorrissen Street, Johannesburg 2050, South Africa

J. H. Potgieter (✉)
Manchester Metropolitan University, Manchester, UK
e-mail: herman.potgieter@wits.ac.za

Introduction

A very important aesthetic quality of textiles in the modern world today is colour. Manufacturing and the use of various dyes are well-established industrial processes. However, the toxic nature of these dyes is becoming a growing environmental concern which needs to be addressed. Synthetic dyes are released from a variety of industries such as textiles, paper, pulp and dyestuff manufacturing (Banerjee et al. 2014), making them one of the largest environmental polluters. Sun et al. (2010) reports that dyes account for approximately 100 tons of waste annually. According to the World Health Organization, by 2025 half of the world's population will be living in water-scare areas (WHO 2017). Given these current water shortage problems and poor water quality, especially in Africa, the organic pollutants released from residual dye effluents are threatening the long-term sustainability of water. In addition to dye effluents being aesthetically unappealing, they have high chemical and biological oxygen demands (Robinson et al. 2001). These organic pollutants are toxic to aquatic life as potentially carcinogenic and mutagenic compounds are produced which are exceptionally harmful to the environment (Banat et al. 1996). Given these harmful effects, dye removal techniques are an essential and necessary step in wastewater treatment.

Residual dyes in wastewater effluents make conventional treatment methods difficult for numerous

Published online: 11 May 2020

reasons, owing to their complex aromatic structure which is resistant to microbial degradation. This can result in treated effluents still being highly coloured (Visa et al. 2010). Multiple treatment methods are commercially available, and one such method that is commonly implemented is adsorption. It has been proved to be one of the most effective ways of colour removal due to simplicity and ease of operation (Ghaedi et al. 2012). However, adsorbents such as activated carbon are often costly, making this technique unattractive. This has promoted research into the use of other low-cost adsorbents such as coal fly ash. Coal fly ash, which is a by-product produced during the combustion of coal in the electricity generation industry accounts for million tons of waste annually worldwide, and in South Africa alone amounts to more than 30 million tons annually (Escom 2017). If viable for colour removal, it would be an excellent low-cost adsorbent. This adsorbent is available in abundance and is creating an environmental concern by being disposed of in landfill sites. Coal fly ash is currently being investigated as an adsorbent using batch configuration under various operating conditions such a pH, temperature, stirring speed, adsorbent dosage and initial dye concentration. It was found to have good adsorption capacity due to the presence of SiO_2, TiO_2 and the remaining unburnt carbon content in the ash (Mohan et al. 2002; Wang and Wu 2006). Studies have shown that pre-treatment of the coal fly ash using physical and chemical methods can improve the adsorption capacity, although this would increase the operating costs of such procedures (Wang and Zhu 2005). Banerjee et al. (2014) investigated the adsorption of methylene blue using acid-activated coal fly ash, which was found to have a high adsorption capacity. Wang et al. (2006) evaluated the effect of NaOH to modify coal fly ash for methylene blue removal and found a 25% increase in its adsorption capacity.

Dye removal techniques have been researched extensively over the past few years; however, very few of these techniques have been implemented by wastewater treatment companies owing to the high cost, low efficiency and inapplicability for a variety of dyes. The current research aims to address this problem and pose a cost-effective, efficient manner of colour removal using a cheap, widely available adsorbent.

This work is beneficial as the removal of an anionic dye has seldom been investigated. Batch configurations have been investigated extensively; however, few studies have been conducted to investigate the adsorption capacity using a continuous column operation or heap adsorption. These operating configurations could potentially have lower operating costs, higher adsorption capacities and be more efficient on a larger scale. The present work also determined the process activation energy, thermodynamic parameters, adsorption isotherms and kinetics using methyl orange (MO) dye.

Materials and methods

Adsorbate (methyl orange)

All chemicals and reagents used were of analytical reagent (AR) grade and were used without further purification. MO is an anionic azo dye available as bright orange crystals and was obtained from ACE Chemicals. MO stock solution (1000 mg l^{-1}) was prepared by dissolving 1 g in 1000 ml of distilled water, and working solutions of 1–14 mg l^{-1} were prepared daily using serial dilution.

Adsorbent (coal fly ash)

Coal fly ash was obtained from the Lethabo power station in South Africa. The coal fly ash was washed with distilled water to remove soluble inorganic material and surface dust particles. Characterization of the coal fly ash was done through XRD and XRF. The elemental composition is summarized in Table 1.

XRD analysis was conducted using a Bruker D2 Phaser X-ray Diffractometer quipped with Cu K α X-Ray source operating at 30 kV and 10 mA. From Fig. 1, the XRD pattern indicates that the mineral phases of the coal fly ash consist of quartz and mullite. The broad peak observed between 2 $\theta = 2°$ and 2 $\theta = 30°$ indicates that the amorphous phases in the coal fly ash contributes more than 50% of the total mass. This amorphous phases consists of silica and alumina in a glass matrix. The Lethabo coal fly ash has been analysed with regards to only major and minor elements. The analysis has not considered the effect of trace amounts of heavy metals. However, the coal fly ash does not contain any significant amounts of heavy

Table 1 Lethabo fly ash composition

Composition	Percentage (%)
SiO_2	52.59
Al_2O_3	34.59
Fe_2O_3	3.15
TiO_2	1.68
MnO	0.04
MgO	1.06
CaO	4.08
Na_2O	0.17
K_2O	0.60
P_2O_5	0.28
Cr_2O_3	0.04
NiO	0.02
V_2O_5	0.04
ZrO_2	0.08
LOI	1.4

metals or radioactive substances. The presence of these elements is dependent on the geological source of the coal used. Specifically, in South Africa this coal fly ash is widely used in the cement making industry, thus implying it is safe to use (Potgieter et al. 2002). Studies have also found that during the cement making process, cement addition had positive effect on the immobilization of heavy metals. However, heavy metal leaching is not a concern in the treated wastewater, except if the pH of the effluent is highly acidic (Wang et al. 2016; Madzivire et al. 2017; Izquierdo and Querol 2012).

Analysis of Lethabo coal fly ash was done by Van der Merwe et al. (2014). Particle size distribution analysis found the mean particle size to be 4.9 µm with 90% of the sample by volume having a particle size smaller than 14.9 µm. The surface area found using Brunauer–Emmett–Teller (BET) analysis was found to be 1.52 $m^{2\ g-1}$.

0.2.3 Batch adsorption tests

Batch adsorption tests were conducted using 5 g of coal fly ash in 150 ml of dye solution at a solid-to-liquid ratio of 1:30. The mixture was continually agitated at a speed of 400 rpm using a magnetic stirrer. Continuous readings were taken for an hour and equilibrium readings after a period of 24 h. The mixture was centrifuged to remove residual adsorbent particles and the absorbance measured. Residual dye concentrations were calculated using a calibration curve prepared at the maximum wavelength of 464 nm with a SQ-2800 UV–Vis spectrophotometer.

Dye concentrations below 4.3×10^{-2} mM were prepared to ensure that the absorbance remained below 1 and within the linear range of the calibration curve. This process was repeated over a range of temperatures (25–45 °C) in order to determine the rate constants and order of the reaction. Adsorption isotherms were determined in a similar manner by varying the absorbent dosage from 3–20 g. All other parameters such as pH, temperature and agitation speed remained constant, and only one variable was varied at a time. The amount of dye adsorbed at equilibrium (q_e) as well as the removal percentages were calculated using Eqs. (1) and (2)

$$q_e = \frac{(C_o - C_e)V_{Sol}}{W} \quad (1)$$

$$\text{Removal } \% = \frac{(C_o - C_e)}{C_O} \times 100\% \quad (2)$$

where C_o and C_e are the initial and equilibrium dye concentrations (mg l^{-1}), W is the mass of adsorbent (g) and V is the volume of dye solution (l). Similarly, from the batch adsorption tests the adsorption kinetics, isotherms and thermodynamic parameters can be determined.

Column adsorption tests

Column adsorption tests were conducted using the same dye concentrations as that of the batch tests. Columns were set up using burettes packed with coal fly ash, ranging from 3–20 g, of varying bed heights between 5 and 40 cm. The column had an internal diameter 1.5 cm. Dye solution was continuously added and allowed to pass through the column. A solid-to-liquid ratio of 1:5 was used.

Heap adsorption tests

Heap adsorption tests were conducted using 180 g of coal fly ash. Dye solution was continuously sprayed on the surface of the coal fly ash. Three washing cycles

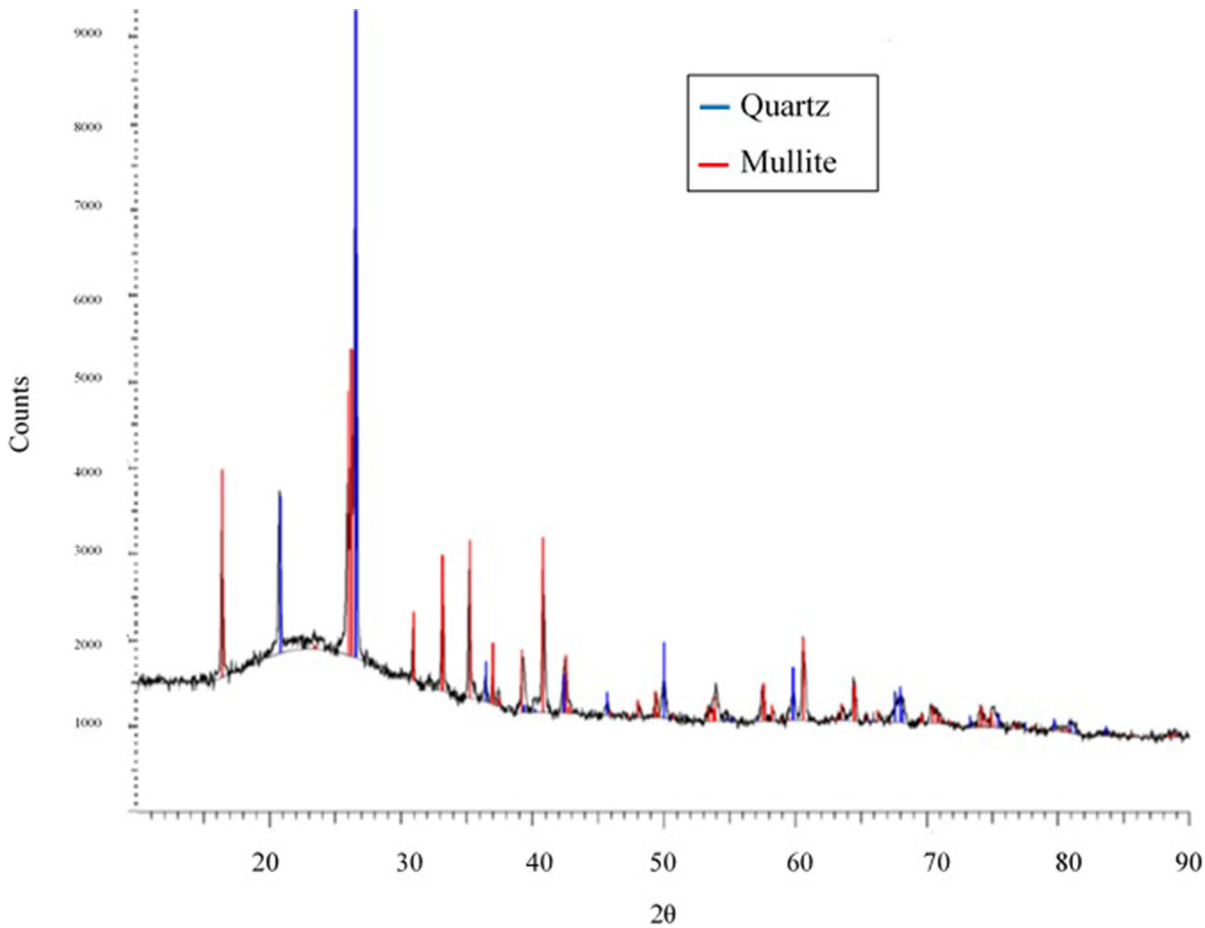

Fig. 1 XRD Analysis of Lethabo fly ash

were used per batch of coal fly ash with a solid-to-liquid ratio of 1:5.

Results and discussion

Preliminary experimental runs were conducted in triplicate to ensure reproducibility and due to good reproducibility; the remaining experiments were conducted in duplicate and mean data values were used for analysis. A preliminary experimental run was also conducted under UV light; however, no significant change in results was observed. The latter experimental runs were conducted at ambient conditions.

Effect of temperature

Batch adsorption tests were conducted in the range of 20–40 °C. Figure 2 shows that the dye removal percentages increase with an increase in temperature which indicates that the adsorption process is endothermic in nature. This may be attributed to the increased mobility of the dye molecules and an increase in the number of active sites due to the temperature increase. Higher temperatures are also known to cause an enlargement of pore size of the remaining active carbon present in the coal fly ash, which increases the adsorption capacity (Senthilkumaar et al. 2006).

Adsorption kinetics

Batch adsorption tests were used to determine the adsorption kinetics, namely whether the process follows Lagergren pseudo-first-order kinetics (Lagergren 1898) or pseudo-second-order kinetics (Ho and McKay 1999) as evaluated according to Eqs. (3) and (4), respectively.

$$\ln(q_e - q_t) = \ln(q_e) - k_1 t \quad (3)$$

$$\frac{t}{q_t} = \left(\frac{1}{k_2}\right)\left(\frac{1}{q_e^2}\right) + \frac{1}{q_e} t \quad (4)$$

where q_e is the amount of dye adsorbed at equilibrium (mg g^{-1}), q_t is the amount of dye adsorbed at time t (mg g^{-1}), k_1 is the pseudo first order rate constant (min^{-1}), and k_2 is second order rate constant (g mg^{-1} min^{-1}). A linear plot of $\ln(q_e - q_t)$ versus t will yield a straight line of slope equal to k_1 and intercept equal to $\ln(q_e)$ if the adsorption follows pseudo-first-order kinetics. A linear plot of $\frac{t}{q_t}$ versus t will yield a straight line of slope equal to $\frac{1}{q_e}$ and intercept equal to $\frac{1}{k_2 q_e^2}$ if the adsorption follows pseudo-second-order kinetics. Lagergren plots for different temperatures were plotted in Figs. 3 and 4 below. It can be seen that the pseudo-second-order plot follows a linear profile the entire operating period with a good correlation coefficient ($R^2 > 0.99$). The first-order plot does not follow a linear profile. This is expected as generally only the initial contact period of approximately 30 min follows a linear relationship (Umpuch and Sakaew 2013). It is also seen that the rate constant decreases with an increase in temperature which is expected for physisorption processes (Tunali et al. 2006). Table 2 summarizes the Lagergren model parameters.

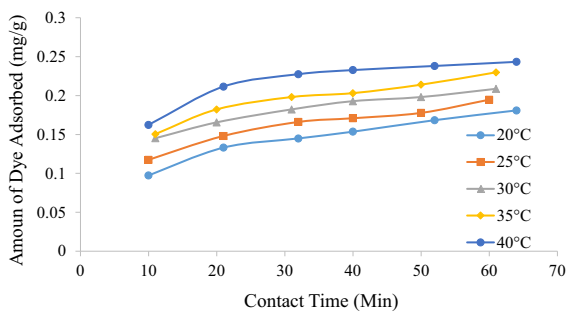

Fig. 2 Effect of temperature of MO adsorption on fly ash

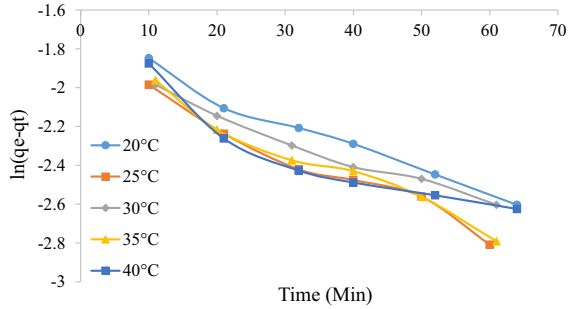

Fig. 3 Lagergren first-order plot for the adsorption of MO at various temperatures

Adsorption isotherms

Adsorption studies are important for solid–liquid processes as this determines the interaction between the adsorbent and adsorbate. The adsorption isotherms were analysed according to the Langmuir, Freundlich and Tempkin models.

Langmuir isotherm

The Langmuir model is used to model monolayer and uniform adsorption on finite adsorption sites. It is also assumed that the adsorbed molecules do not interact with neighbouring sites (Belhachemi and Addoun 2011). The Langmuir model is represented by Eq. (5) (Langmuir 1916).

$$\frac{C_e}{q_e} = \frac{C_e}{q_m} + \frac{1}{k_L q_m} \quad (5)$$

where q_e is the maximum adsorption capacity at equilibrium (mg g^{-1}), C_e is equilibrium concentrations of the adsorbate (mg l^{-1}), q_m is the theoretical maximum adsorption capacity for the process

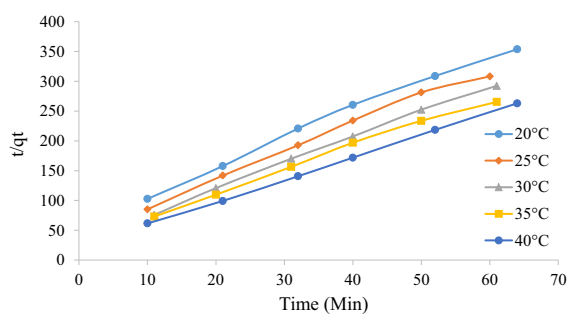

Fig. 4 Lagergren pseudo-second-order plot for the adsorption of MO at various temperatures

Table 2 Lagergren first-order and pseudo-second-order kinetic adsorption parameters

	Lagergren first order			Lagergren pseudo second order		
	k_1 (min^{-1})	R^2	q_e	k_2 (g mg^{-1} min^{-1})	R^2	q_e
20 °C	0.013	0.9805	0.17	0.33	0.9929	0.22
25 °C	0.017	0.9671	0.15	0.27	0.9909	0.24
30 °C	0.012	0.9796	0.15	0.23	0.998	0.26
35 °C	0.015	0.9674	0.16	0.21	0.9951	0.27
40 °C	0.12	0.8379	0.15	0.18	0.9996	0.30

(mg g^{-1}), k_L is the Langmuir adsorption constant related to the free energy of adsorption (l mg^{-1}). A plot of $\frac{C_e}{q_e}$ versus C_e will yield a straight line of slope equal to $\frac{1}{q_m}$ and intercept equal to $\frac{1}{k_L q_m}$ if Langmuir adsorption prevails.

Freundlich isotherm

The Freundlich model thoroughly represents multilayer adsorption on heterogeneous surfaces. It is not restricted to the formation of the monolayer and is represented by Eq. (6) (Freundlich 1906).

$$\ln q_e = \ln K_F + \left(\frac{1}{n}\right) \ln C_e \tag{6}$$

where K_F is a Freundlich constant indicative of the relative adsorption capacity of the adsorbent (mg g^{-1}), $\frac{1}{n}$ is the heterogeneity factor indicating the favourability and capacity of the system (Piccin et al. 2011). A value of $n < 1$ indicates unfavourable adsorption, $n > 1$ indicates favourable adsorption and equal to 1 indicates the adsorption process is linear. A plot of $\ln q_e$ versus $\ln C_e$ will yield a straight line of slope equal to $\frac{1}{n}$ and intercept equal to $\ln K_F$ from which the constants can be determined if the process obeys the Freundlich isotherm.

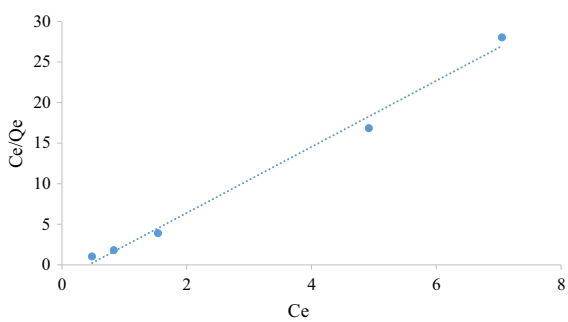

Fig. 5 Langmuir batch isotherm

Temkin isotherm

The Temkin model considers the effects of some indirect adsorbate/adsorbate interactions in adsorption isotherms (Piccin et al. 2011). The Temkin model is presented by Eq. (7).

$$q_e = \frac{RT}{b} \ln K_T + \frac{RT}{b} \ln C_e \tag{7}$$

where KT is the equilibrium binding constant (l mol^{-1}), b is a constant related to adsorption heat (J mol^{-1}), R is the universal gas constant (8.314 J mol^{-1} K^{-1}), and T is the absolute temperature (K). A plot of q_e versus $\ln C_e$ will yield a straight line of slope equal to $\frac{RT}{b}$ and intercept equal to $\frac{RT}{b} \ln K_T$ from which the constants can be determined if the adsorption follows the Temkin model.

Figures 5, 6, 7, 8, 9 and 10 show the respective Langmuir, Freundlich and Temkin isotherms with a variation in adsorbent dosages (1.5–20 g) at neutral pH and 22 °C when using batch and column configurations. Upon closer inspection of the R^2 value, the Freundlich model most accurately represents the adsorption process of both the batch and column configuration. However, the Langmuir model also has a good R^2 value. However, due to a negative slope resulting in a negative value of the Langmuir constant (k_L) being physically impossibly, this model is not an accurate representation and the adsorption does not follow this isotherm (Kiurski et al. 2011). The constant, n, from the Freundlich model is greater than 1, which indicates favourable adsorption. The negative value of the Temkin constant, which signifies the heat of adsorption, also indicates that the process is endothermic. The constant parameters were all determined by the respective isotherm plots and are summarized in Table 3.

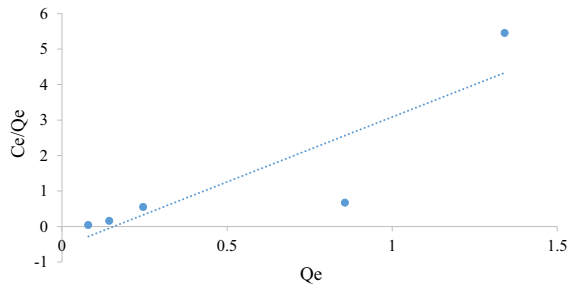

Fig. 6 Langmuir column isotherm

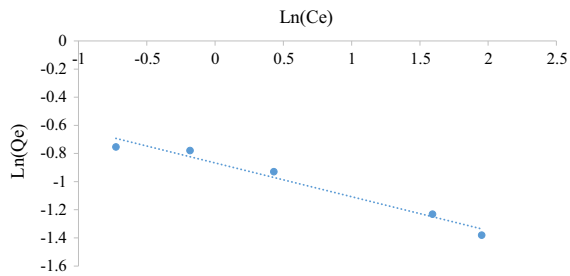

Fig. 7 Freundlich batch isotherm

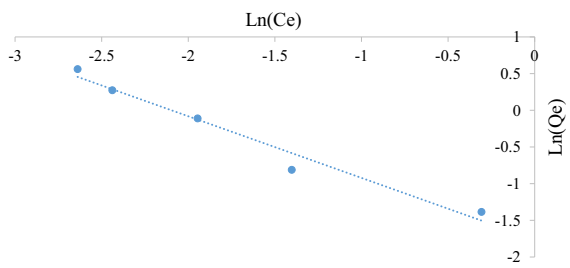

Fig. 8 Freundlich column isotherm

Thermodynamics

The thermodynamics of the adsorption process can be analysed in order to determine the mechanism, such as whether the process is physical or chemical,

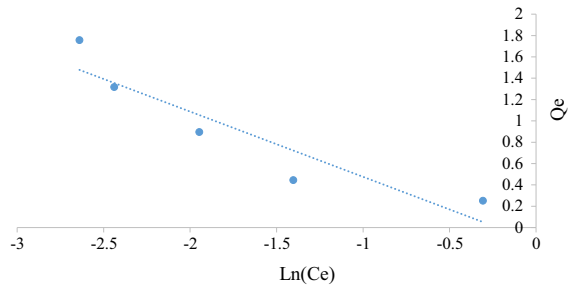

Fig. 9 Tempkin batch isotherm

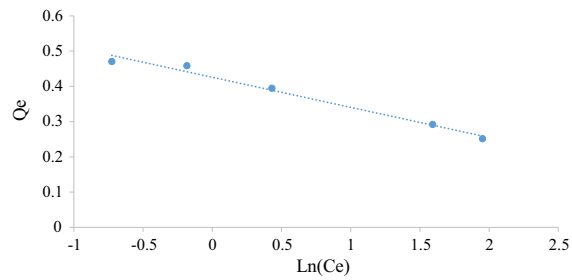

Fig. 10 Tempkin column isotherm

spontaneous or non-spontaneous and exothermic or endothermic. Adsorption studies need to be conducted at different temperatures in order to determine parameters such as the activation energy (E_a), change in standard free energy ($\Delta G°$), enthalpy ($\Delta H°$) and entropy ($\Delta S°$). These parameters can be estimated using Eqs. (8), (9) and (10).

$$K_C = \frac{q_e}{C_e} \tag{8}$$

$$\ln K_c = \frac{\Delta S^{\circ}}{R} - \frac{\Delta H^{\circ}}{RT} \tag{9}$$

$$\Delta G^{\circ} = -RT \ln K_c \tag{10}$$

Table 3 Langmuir, Freundlich and Tempkin adsorption isotherm constants

	Langmuir			Freundlich			Tempkin		
	k_L	q_m (mg g^{-1})	R^2	k_F (mg/g)	n	R^2	k_T	b (kJ/mol)	R^2
Batch	− 2.32	0.25	0.9923	0.42	4.16	0.969	1	− 29.00	0.982
Column	− 0.69	0.69	0.7608	0.17	1.19	0.9694	1	− 4.10	0.8558

Table 4 Thermodynamic parameters for the adsorption of MO on fly ash at 25 °C

Temp (°C)	$\Delta G°$ (kJ mol^{-1})	$\Delta H°$ (kJ mol^{-1})	$\Delta S°$ (kJ mol^{-1})
20	− 9.36	13.36	77.75
25	− 9.84		
30	− 10.29		
35	− 10.68		
40	− 10.88		

where R is the universal gas constant (8.314 J mol^{-1} K^{-1}), T is the absolute temperature (K), $\Delta H°$ is the standard enthalpy (kJ mol^{-1}), $\Delta S°$ is the standard entropy (kJ mol^{-1}), and $\Delta G°$ is the standard free energy change (kJ mol^{-1}). Values for $\Delta H°$ and $\Delta S°$ can be calculated from the slope and intercept of a linear plot of $\ln K_c$ and $\frac{1}{T}$ (Banerjee et al. 2013). Estimated values for these parameters are tabulated and shown in Table 4.

The negative value of $\Delta G°$ for all temperatures indicates that the adsorption process is spontaneous. The positive $\Delta H°$ value as well as the increase in $\Delta G°$ values with an increase in temperature further shows the process is endothermic, as adsorption is favoured at higher temperatures. This is most likely due to the fact that the mobility of the adsorbate increases with an increase in temperature and the affinity of the adsorbate increases at higher temperatures (Saha and Chowdhury 2011). A positive $\Delta S°$ suggests that the process follows a dissociative mechanism, i.e. that there is an affinity of the adsorbent for the adsorbate, as well as an increases in the degree of freedom accompanied by an increase in randomness at the solid–liquid interface (Saha and Chowdhury 2011). The magnitude of $\Delta G°$ and $\Delta H°$ indicates that the process is physical as $\Delta G°$ is in the range of 0–20 kJ mol^{-1} (Salam et al. 2012) and $\Delta H°$ in the range of 2.1–20.9 kJ mol^{-1} (Liu and Liu 2008). Similar findings were obtained by Jalil et al. (2010) and Yang et al. (2016) for other low-cost adsorbents using MO.

The pseudo-second-order rate constants from the Lagergren model (k_2) evaluated at different temperatures using a batch configuration were used to determine the activation energy of the adsorption process by applying the Arrhenius equation given by Eq. (11). A plot of ln k versus $\frac{1}{T}$ is shown in Fig. 11.

$$\ln k_2 = \ln A - \frac{E_a}{RT} \tag{11}$$

where E_a is the activation energy (kJ mol^{-1}) and A is the Arrhenius factor (g mol^{-1} s^{-1}).

The activation energy was calculated to be − 20.82 kJ mol^{-1}. This value is fairly small, which is an indication that the adsorption may not be very sensitive to the experimental temperature range. The low value ($E_a < 42$ kJ mol^{-1}) indicates that the adsorption is physical (Umpuch and Sakaew 2013). The negative activation energy implies that the rate of adsorption decreases with an increase in temperature which leads to a reduction in the probability of the colliding molecules being captured by the adsorbent. This negative value also indicates that energy barriers are absent in this process (Kobiraj et al. 2012).

Column, batch and heap adsorption comparison

Figure 12 shows the dye removal comparison between batch and column operation using the same solution volume, adsorbent dosage as well as pH.

It can be seen that the column configuration has a much larger dye removal percentage. This high removal efficiency on the column operation was largely dependent on the bed height, with the largest adsorbent dosage having the greatest removal efficiency due to longer residence times and increased number of binding sites (Olgun et al. 2013). Removal percentages became stagnant beyond a certain mass of adsorbent as binding sites were restricted due to tight column packing (Chen et al. 2011).

Heap adsorption showed an overall dye removal of 99.25% after 3 washing cycles compared to a column with a maximum removal of 99.95% and batch with 96.68%. Both the column and heap adsorption are comparable in performance. Each configuration has their own drawbacks, as heap adsorption requires a large adsorbent mass and area, whereas column operations have long residence times and batch operations are energy intensive.

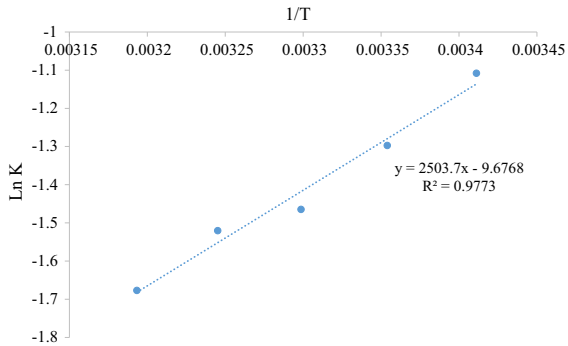

Fig. 11 Activation energy plot for the adsorption on MO on fly ash

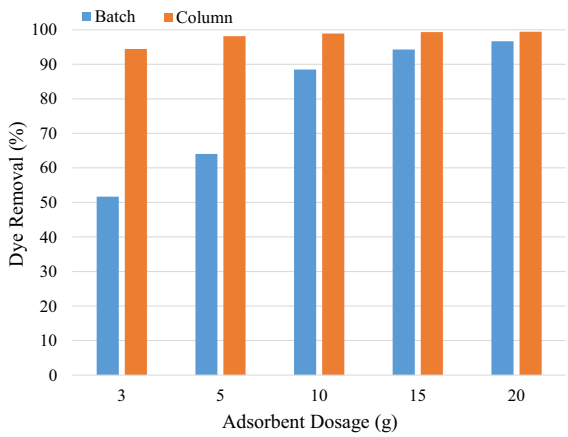

Fig. 12 Dye removal comparison between batch and column configurations

Adsorption capacity

The maximum adsorption capacity of the column (8.9 mg g^{-1}) is higher than that of the batch process (3.9 mg g^{-1}) under the same operating conditions. This may be due to the surface of coal fly ash, which favours solid-state diffusion relative to the batch configuration. Similar results of higher column adsorption capacities were reported by (Gupta et al. 2001). Heap adsorption has an intermediate adsorption capacity of 4.0 mg g^{-1}. Fairly low adsorption capacities are indicative of an anionic dye since the presence of a negatively charged carboxyl group, which is an important functional group present in industrial effluents, inhibits the adsorption of anionic dyes (Gong et al. 2005). Table 5 shows a comparison of adsorption capacities found by similar studies using an anionic dye under batch configuration.

Adsorption capacities differ drastically due to different sample pre-treatment, pH, contact times and temperatures. One major difference is the particle size of the coal fly ash. Since a small surface area of 1.42 m^2 g^{-1} was found, there were less active sites present for adsorption resulting in the low adsorption capacity. However, in comparison, the adsorption capacity of coal fly ash is in a fairly intermediate range and can be considered a viable alternative for dye removal.

Table 5 Adsorption capacity comparison between varying adsorbents and anionic dyes

Adsorbent	Anionic dye	Adsorption capacity (mg g^{-1})	References
Fly ash	Methyl orange	3.9	Present study
Fly ash	Reactive blue 171	3.75	Banerjee et al. (2014)
Carbon nanotubes	Methyl orange	44.16	Zhao et al. (2013)
Peanut Hull	Sunset yellow	13.99	Wang and Zhu (2005)
Coal fly ash-NaOH	Acid red 1	12.66	Hsu (2008)
Fly ash	Acid red 91	1.75	Ramakrishna and Viraraghavan (1997)
Chitosan beads	Remazol blue	201.6	Pereira et al. (2017)
Cross-linked chitosan	Methyl orange	89.29	Huang et al. (2017)
Eggshells	Congo red	49.5	Abdel-Khalek et al. (2017)
ZnO nanoparticles	Congo red	71.43	Kataria and Garg (2017)

Table 6 Economic evaluation for various operating conditions

	Batch	Column	Heap leaching
Maximum adsorption capacity (mg/g)	3.9	8.9	4.0
Mass of fly ash required (Tonnes/Day)	128	56	125
Cost of treatment (R/day)	2500	1094	2441

Economic evaluation

Despite column operation being the most efficient dye removal technique, each method has various economic constraints. On the assumption that 100 Ml of water needs to be treated daily, with dye concentration of 500 ppm to be reduced to 1 ppm, Table 6 summarizes the costs and mass required for each operation. Coal fly ash was assumed to have no cost associated with it, and only logistical costs such as transportation need to be considered and were estimated based on the mass of adsorbent required (Freight Rate Calculator 2017). The mass of coal fly ash required is determine from the respective adsorption capacities.

Column operation is the cheapest due to the smaller adsorbent dosage required. Various government grants in South Africa are awarded to wastewater treatment plants such as the Regional Bulk Infrastructure Grant which allocates an excess of 5 billion rand to various wastewater treatment companies (van Zyl et al. 2016). Other revenue sourced from industries is the premium paid to treat or dispose wastewater effluents. While the use of coal fly ash seems feasible, further studies at larger scale, such as a pilot plant, needs to be conducted.

Conclusions

The study shows that coal fly ash, which is often applied for cationic dye removal, is also a suitable adsorbent for the removal of the anionic dye, methyl orange. The adsorption process follows pseudo-second-order kinetics and the Freundlich isotherm most accurately represents the adsorption for both batch and column configurations. Upon analysis of the thermodynamic parameters, negative values of the Gibbs free energy change indicate the process is spontaneous. Positive enthalpy and entropy changes indicate that the adsorption is endothermic, random and a physical process. The adsorption process has an activation energy of -20.82 kJ mol^{-1}, suggesting that energy barriers are very low or absent. Of the three configurations, dye adsorption is the highest using column operation, followed by heap adsorption and lastly a batch operation.

Acknowledgements The University of the Witwatersrand is acknowledged for financial and technical support throughout the research.

Open Access This article is licensed under a Creative Commons Attribution 4.0 International License, which permits use, sharing, adaptation, distribution and reproduction in any medium or format, as long as you give appropriate credit to the original author(s) and the source, provide a link to the Creative Commons licence, and indicate if changes were made. The images or other third party material in this article are included in the article's Creative Commons licence, unless indicated otherwise in a credit line to the material. If material is not included in the article's Creative Commons licence and your intended use is not permitted by statutory regulation or exceeds the permitted use, you will need to obtain permission directly from the copyright holder. To view a copy of this licence, visit http://creativecommons.org/licenses/by/4.0/.

References

Abdel-Khalek, M. A., Rahman, M. K. A., & Francis, A. A. (2017). Exploring the adsorption behavior of cationic and anionic dyes on industrial waste shells of egg. *Journal of Environmental Chemical Engineering*, *5*, 319–327. https://doi.org/10.1016/j.jece.2016.11.043.

Banat, I. M., Nigam, P., Singh, D., et al. (1996). Microbial decolourisation of textile-dye containing effluents: A review. *Bioresources Technology, 58*, 217–227.

Banerjee, S., Nigam, V., & Chattopadhyaya, M. (2013). Effective adsorption of anionic dye, ORANGE G, from aqueous solutions onto activated carbon derived from saw dust by chemical activation with perchloric acid. *Journal of the Indian Chemical Society, 90*, 1211–1221.

Banerjee, S., Sharma, G. C., Chattopadhyaya, M. C., et al. (2014). Kinetic and equilibrium modelling for the adsorptive removal of methylene blue from aqueous solutions on of activated fly ash (AFSH). *Journal of Environmental Chemical Engineering, 2*, 1870–1880.

Belhachemi, M., & Addoun, F. (2011). Comparative adsorption isotherms and modelling of methylene blue onto activated carbons. *Applied Water Science, 1*, 111–117.

Chen, N., Zhang, Z., Feng, C., et al. (2011). Investigations on the batch and fixed-bed column performance of fluoride adsorption by Kanuma mud. *Desalination, 268*, 76–82.

Eskom and ash management. Eskom. (2017) [cited 2017 Sep 9]. https://www.eskom.co.za/news/Pages/Feb20.aspx. Accessed 15 Oct 2018.

Freight Rate Calculator. Freightos. (2017) [cited 2017 Oct 18]. https://www.freightos.com/portfolio-items/freight-rate-calculator-free-tool/. Accessed 15 Oct 2018.

Freundlich, H. (1906). Over the adsorption in solution. *Journal of Physical Chemistry, 57*, 1100–1107.

Ghaedi, M., Sadeghian, B., Pebdani, A. A., et al. (2012). Kinetics, thermodynamics and equilibrium evaluation of direct yellow 12 removal by adsorption onto silver nanoparticles loaded activated carbon. *Chemical Engineering Journal, 187*, 133–141.

Gong, R., Ding, Y., Li, M., et al. (2005). Utilization of powdered peanut hull as biosorbent for removal of anionic dyes from aqueous solution. *Dyes & Pigments, 64*, 187–192.

Gupta, V. K., Gupta, M., & Sharma, S. (2001). Process development for the removal of lead and chromium from aqueous solutions using red mud—an aluminium industry waste. *Water Research, 35*, 1125–1134.

Ho, Y. S., & McKay, G. (1999). Pseudo-second order model for sorption processes. *Process Biochemistry, 34*, 451–465.

Hsu, T.-C. (2008). Adsorption of an acid dye onto coal fly ash. *Fuel*, *87*, 3040–3045.

Huang, J., Xu, C., Ridoutt, B. G., Wang, X., & Ren, P. (2017). Nitrogen and phosphorus losses and eutrophication potential associated with fertilizer application to cropland in China. *Journal of Cleaner Production*, *159*, 171–179. https://doi.org/10.1016/j.jclepro.2017.05.008.

Izquierdo, M., & Querol, X. (2012). Leaching behaviour of elements from coal combustion fly ash: An overview. *International Journal of Coal Geology, 94*, 54–66.

Jalil, A. A., Triwahyono, S., Adam, S. H., et al. (2010). Adsorption of methyl orange from aqueous solution onto calcined Lapindo volcanic mud. *Journal of Hazardous Materials, 181*, 755–762.

Kataria, N., & Garg, V. K. (2017). Removal of Congo red and Brilliant green dyes from aqueous solution using flower shaped ZnO nanoparticles. *Journal of Environmental Chemical Engineering*, *5*, 5420–5428. https://doi.org/10.1016/j.jece.2017.10.035.

Kiurski, J., Adamovic, S., Krstic, J., et al. (2011). Adsorption efficiency of low-cost materials in the removal of Zn (II) ions from printing developer. *Acta Technica Corviniensis-Bulletin of Engineering, 4*, 61–67.

Kobiraj, R., Gupta, N., Kushwaha, A. K., et al. (2012). Determination of equilibrium, kinetic and thermodynamic parameters for the adsorption of Brilliant Green dye from aqueous solutions onto eggshell powder. *Indian Journal of Chemical Technology, 19*, 26–31.

Lagergren, S. (1898). *About the theory of so-called adsorption of soluble substances*. Vetenskapsakademiens: K. Sven.

Langmuir, I. (1916). The constitution and fundamental properties of solids and liquids. Part I. Solids. *Journal of the American Chemical Society, 38*, 2221–2295.

Liu, Y., & Liu, Y.-J. (2008). Biosorption isotherms, kinetics and thermodynamics. *Separation and Purification Technology, 61*, 229–242.

Madzivire, G., Ramasenya, K., Tlowana, S., et al. (2017). Application of mine water leaching protocol on coal fly ash to assess leaching characteristics for suitability as a mine backfill material. *Journal of Environmental Science and Health Part A*, *53*(5), 467–474.

Mohan, D., Singh, K. P., Singh, G., et al. (2002). Removal of dyes from wastewater using fly ash, a low-cost adsorbent. *Industrial and Engineering Chemistry Research, 41*, 3688–3695.

Olgun, A., Atar, N., & Wang, S. (2013). Batch and column studies of phosphate and nitrate adsorption on waste solids containing boron impurity. *Chemical Engineering Journal, 222*, 108–119.

Pereira, F. A. R., Sousa, K. S., Cavalcanti, G. R. S., et al. (2017). Green biosorbents based on chitosan-montmorillonite beads for anionic dye removal. *Journal of Environmental Chemical Engineering*, *5*, 3309–3318. https://doi.org/10.1016/j.jece.2017.06.032.

Piccin, J., Dotto, G., & Pinto, L. (2011). Adsorption isotherms and thermochemical data of FD&C Red N40 binding by chitosan. *Brazilian Journal of Chemical Engineering, 28*, 295–304.

Potgieter, J. H., Potgieter, S. S., Loubser, M., et al. (2002). Stabilisation of a ferro-industry waste in various solid matrices. *Journal of Chemical Technology and Biotechnology, 77*, 311–314.

Ramakrishna, K. R., & Viraraghavan, T. (1997). Dye removal using low cost adsorbents. *Water Science and Technology*, *36*, 189–196.

Robinson, T., McMullan, G., Marchant, R., et al. (2001). Remediation of dyes in textile effluent: A critical review on current treatment technologies with a proposed alternative. *Bioresources Technology, 77*, 247–255.

Saha P, Chowdhury S. (2011). *Insight into adsorption thermodynamics* (Vol. 450). InTech

Salam, M. A., Gabal, M. A., & Obaid, A. Y. (2012). Preparation and characterization of magnetic multi-walled carbon nanotubes/ferrite nanocomposite and its application for the removal of aniline from aqueous solution. *Synthetic Methods, 161*, 2651–2658.

Senthilkumaar, S., Kalaamani, P., & Subburaam, C. (2006). Liquid phase adsorption of crystal violet onto activated carbons derived from male flowers of coconut tree. *Journal of Hazardous Materials, 136*, 800–808.

Sun, D., Zhang, X., Wu, Y., et al. (2010). Adsorption of anionic dyes from aqueous solution on fly ash. *Journal of Hazardous Materials, 181*, 335–342.

Tunali, S., Özcan, A. S., Özcan, A., et al. (2006). Kinetics and equilibrium studies for the adsorption of Acid Red 57 from aqueous solutions onto calcined-alunite. *Journal of Hazardous Materials, 135*, 141–148.

Umpuch, C., & Sakaew, S. (2013). Removal of methyl orange from aqueous solutions by adsorption using chitosan intercalated montmorillonite. *Songklanakarin Journal of Science and Technology, 35*, 451–459.

Van der Merwe, E. M., Mathebula, C., & Prinsloo, L. C. (2014). Characterization of the surface and physical properties of South African coal fly ash modified by sodium lauryl

sulphate (SLS) for applications in PVC composites. *Powder Technology, 266*, 70–78.

van Zyl, F., Marais, S., & Mokoena, L., et al. (2016). *Provinical regional bulk water infrustructure master plan [internet]*. Department of Water Affairs; (2016) [cited 2017 Oct 17]. https://www.dwaf.gov.za/Downloads/WS/Macro_Planning_Products/PROVINCIAL REGIONAL BULK WATER SANITATION INFRASTRUCTURE MASTER PLAN/2016/NW_Reg_Bulk.pdf. Accessed 15 Oct 2018.

Visa, M., Bogatu, C., & Duta, A. (2010). Simultaneous adsorption of dyes and heavy metals from multicomponent solutions using fly ash. *Applied Surface Science, 256*, 5486–5491.

Wang, X., Li, A., & Zhang, Z. (2016). The effects of water washing on cement-based stabilization of MWSI fly ash. *Procedia Environmental Science, 31*, 440–446.

Wang, S., Soudi, M., Li, L., et al. (2006). Coal ash conversion into effective adsorbents for removal of heavy metals and dyes from wastewater. *Journal of Hazardous Materials, 133*, 243–251.

Wang, S., & Wu, H. (2006). Environmental-benign utilisation of fly ash as low-cost adsorbents. *Journal of Hazardous Materials, 36*, 482–501.

Wang, S., & Zhu, Z. (2005). Sonochemical treatment of fly ash for dye removal from wastewater. *Journal of Hazardous Materials, 126*, 91–95.

World Health Organization Drinking Water [Internet]. WHO. (2017) [cited 2017 Sep 16]. https://www.who.int/mediacentre/factsheets/fs391/en/. Accessed 15 Oct 2018.

Yang, D., Qiu, L., & Yang, Y. (2016). Efficient adsorption of methyl orange using a modified chitosan magnetic composite adsorbent. *Journal of Chemical Engineering Data, 61*, 3933–3940.

Zhao, D., Zhang, W., Chen, C., & Wang, X. (2013). Adsorption of methyl orange dye onto multiwalled carbon nanotubes. *Procedia Environmental Sciences*, *18*, 890–895. https://doi.org/10.1016/j.proenv.2013.04.120.

Publisher's Note Springer Nature remains neutral with regard to jurisdictional claims in published maps and institutional affiliations.